

# Geochemical and mineralogical characteristics of some gold mine tailings in the Eastern Desert of Egypt

Mostafa REDWAN (✉)

Geology Department, Faculty of Science, Sohag University, Sohag 82524, Egypt

© Higher Education Press 2022

**Abstract** The adverse environmental effects of mine tailings disposal on the surrounding ecosystems are worldwide environmental problems. Due to environmental issues related to tailings discharged on land surface, detailed tailings characterization is a prerequisite for a long-term management solution. The tailings from four gold mines in Egypt, namely Fatira, El Sid, Barramiya, and Atud were investigated for their geochemical-mineralogical features and the effect of weathering behavior on the release of their heavy elements. The tailings samples were investigated by mineralogical (XRD and ESEM-EDS), physical (grain-size distribution) and geochemical (XRF) techniques. Most of the tailings have uniform silt-size with fine to very finesand and clay. Atud tailings have coarse to fine sands. High carbonate, predominantly calcite was found for the samples from Fatira and Atud, calcite-ankerite from El Sid and dolomite from Barramiya with little sulfide-content. High-mean of Cr (569287 mg/kg), Ni (89191 mg/kg) and Co (4221 mg/kg) values are coinciding with the ultramafic nature in Atud and Barramiya tailings. El Sid tailings have a high-mean concentration of Zn (1357 mg/kg) and Pb (1349 mg/kg). Barramiya tailings have a high-mean As concentration (2635 mg/kg). The Fatira tailings are characterized by high-mean values of Sr (444 mg/kg) and Cu (280 mg/kg) arising from auriferous mineralization. High Sr concentrations in Fatira tailings are mainly due to its adsorption to iron oxides. Pyrite oxidation is conceded along the cracks and/or the edges of the crystals in the El Sid, Barramiya and Atud tailings. The Threshold Effect Level (TEL) values indicated high contamination from heavy elements to the neighboring ecosystem. The tailings were deposited downstream into the small wadis. Wind and water erosion can dissolve efflorescent materials enriched in toxic elements like As, Zn, and Pb at tailings surface. The release of contaminants could be catastrophic for the environment without mine site rehabilitation strategies.

**Keywords** gold mine, tailings, geochemistry, mineralogy, Egypt

## 1 Introduction

Every year large-scale mining activities generate intense and prolonged environmental impact modifying the entire landscapes by removing and processing billions of tons of rocky materials (Carmo et al., 2020). Mine tailings are the finely ground residues produced from the crushing and grinding of the ore rock matrix to liberate valuable ore minerals (Blowes et al., 2003). Different heavy metal and metalloid contaminants (for example, As, Cd, Cr, Cu, Fe, Pb, and Zn) are associated with gold mine tailings and are treated as one of the major anthropogenic contaminants with enormous hazards that are disturbing environmental ecosystems (Souissi et al., 2015). Extensive water and/or wind erosions of these tailings take place due to the absence of suitable plants (Mendez and Maier, 2008) or multiple-layered dry covers (Redwan and Bamoussa, 2019). These contaminants can enter the human body through inhalation, digestion or even direct contact, and contribute toward a range of illnesses (Helser and Cap-puyns, 2021). Therefore, identifying and characterizing the zones of these hazardous wastes is necessary where huge volumes of these potentially toxic elements can be liberated into the surrounding environment.

Since ancient times, the Eastern Desert of Egypt was widely known as a gold-mining area. There are more than 100 vein-type gold sites extending through Precambrian basement rocks. There has been a total of 400000–600000 tons of quartz ore mined from ancient trenches and underground workings, and supposing a recovery of 10 g/t, yielded a maximum of 6000 kg Au. During the early to mid-20th century (1902–1958), the total obtained gold amounted to around 7 tons (Klemm et al., 2001; Kochin and Bassyuni, 1968).

The exploitation of lower ore grades in modern gold mines caused the growth in volume of tailings produced,

and tailings management has become a crucial part of gold mining activity (Hudson-Edwards et al., 2011). At present, very little literature focuses on the gold tailings detailing geochemical and mineralogical investigations or environmental concerns due to sulfide oxidation and heavy element mobility. The present study focuses on mineralogical, geochemical and environmental aspects of tailings material in four areas in the Eastern Desert of Egypt and the effect of weathering behavior on the contaminant load release.

## 2 Study area

### 2.1 Gold mine tailings

Four mine tailings related to gold mine deposits in the central part of the Eastern Desert of Egypt were selected for further investigation.

#### 2.1.1 Fatira

The Fatira gold mine area and tailings are set in the North Eastern Desert of Egypt (Figs. 1 and 2(a)). It was mined during the New Kingdom, Roman period, by the Fatira Exploring Company from 1902 to 1905, in 1957 by the Egyptian Mining and Prospecting Company and from 1975–1977 by the Egyptian Geological Survey (EMRA). The gold content ranged from 0.6 to 17.09 g/t with a mean of 2.2 g/t (Azzaz et al., 1997). Most mines and settlement localities in the study area are situated in the Wadi Abu Zawal, the eastern tributary of the Wadi Fatira. The major mining sites are located in the mountains between Fatira II and III (Murr, 1999; Klemm and Klemm, 2013). The modes of gold occurrence are found in three phases starting from the weathered dykes of

felsite, great quartz veins penetrating the granitic rocks, and siliceous shear zones trending NNW-SSE and splitting the metavolcanic and granitic rocks (Abd El Monsef et al., 2020). The granodiorite rocks are completely altered around the veins. Plagioclases and alkali feldspars are intensely sericitised. Ideomorphic ores are irregularly located in the quartz. Most ores are found inside chlorite or secondary muscovite. The gold-sulphide complexes decompose due to the interaction between the gold-sulphide structures and the iron wall rock causing the precipitation of gold (Murr, 1999; Klemm and Klemm, 2013).

#### 2.1.2 El Sid

The El Sid gold mine tailings are found mid-way between Qift (Nile Valley) and Quseir (Red Sea coast) (Figs. 1 and 2(b)). El Sid was mined during Pharaonic, Roman, and between 1940–1957. During this last time span, 120000 tons of ore (grade mean 27.9 g/t) provided 3110 kg of gold, with 330000 tons of rock wastes and mill tailings (mean 3 g/t gold) (Kochin and Bassyuni, 1968). A gold vein-type mineralization was formed in sheared ophiolitic ultramafic rocks and in hydrothermal veins of quartz in the granite/serpentinite boundary (Botros, 2004) and on the Fawakhir granite western border which continued west over a wide graphite schist zone (El-Bouseily et al., 1985). Pyrite and arsenopyrite are the prevalent minerals in the mineralized veins (El Ramly et al., 1970), as well as chalcopyrite, sphalerite, and galena (Hussein, 1990).

#### 2.1.3 Barramiya

The Barramiya gold mine tailings are situated mid-way between Mersa Alam (Red Sea coast) and Idfu (Nile Valley) (Figs. 1 and 2(c)). Barramiya was mined during Pharaonic times. It was mined from 1907–1919 by the Baramia Mining and Exploration Company Ltd., with 50211 ounces of gold production (Attia, 1948). The gold content ranged from 2.2 to 15.5 g/t (Hussein, 1990). The gold vein-type mineralization was formed in sheared ophiolitic ultramafic rocks (Botros, 2004). The ophiolitic melange covers up to 75% of the surface rocks and consists of allochthonous serpentinite spread out within highly deformed actinolite and graphite schist (Botros, 2004). The gold veins are confined to the fracture tracts and exist in the graphitic schist. There is little pyrite and chalcopyrite associated with the gold (Hussein, 1990).

#### 2.1.4 Atud

The Atud gold mine is situated in the central part of the Eastern Desert of Egypt (Figs. 1 and 2(d)). The Atud gold mine was exploited during Pharaonic times. Detailed surface and subsurface geological studies were made by the Egyptian Geologic Survey and Mining Authorities



**Fig. 1** Location (Google earth) map of the study area showing the locations of Fatira, El Sid, Barramiya and Atud gold mine areas.

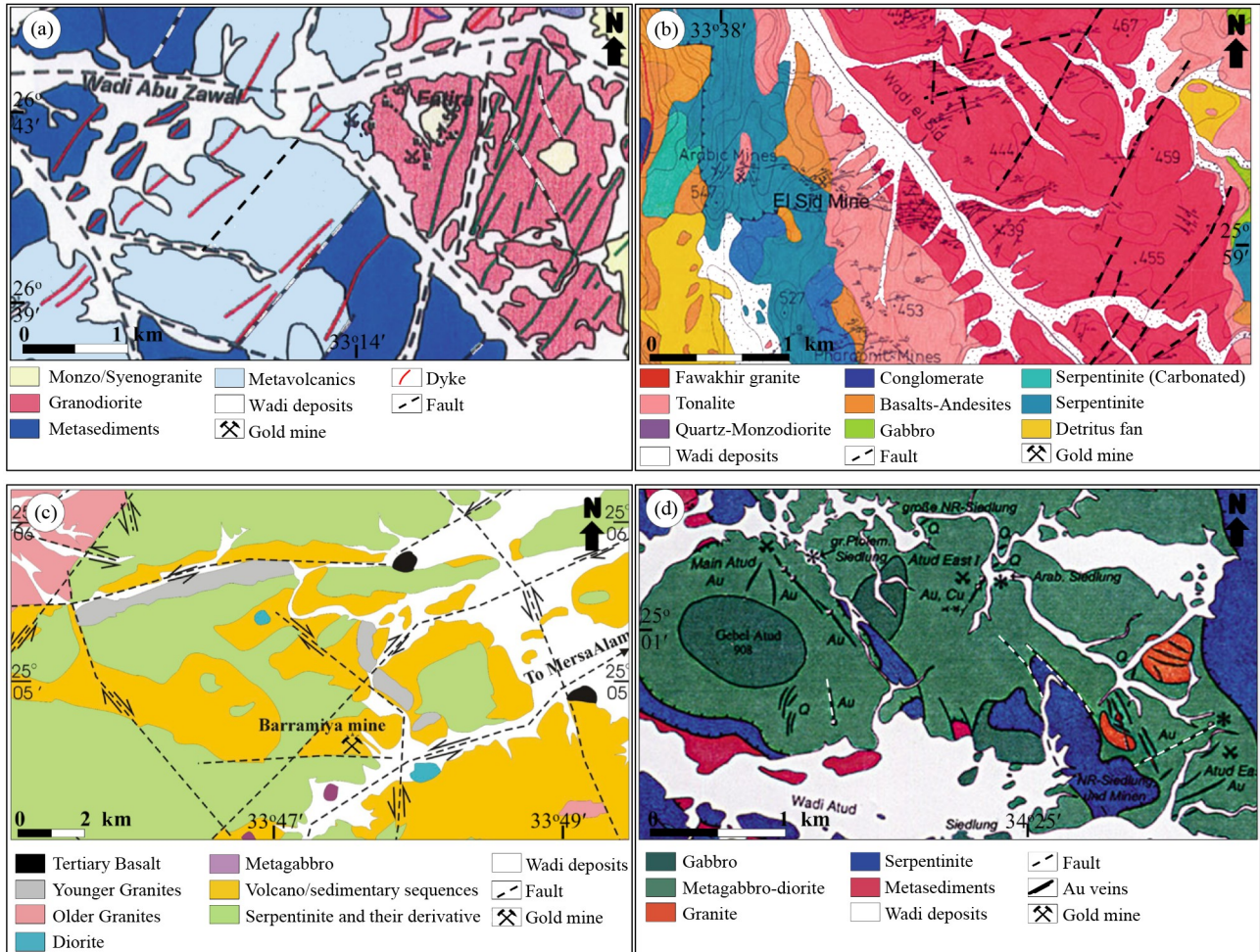


**Fig. 2** Geological maps of (a) Fatira (after Abd El Monsef et al. 2020), (b) El Sid (after Langwieder 1994), (c) Barramiya (after Harraz et al. 2012) and (d) Atud (after Harraz 2002; Klemm and Klemm 2013).

(EGSMA) between 1953 and 1969 (Gabra, 1986). The gold content in the area ranged from 0.1 to 31 g/t with a mean of 16.28 g/t. There were 19000 tons of rock and 348 kg of pure gold extracted from the main vein (Gabra, 1986). There were about 1600 tons of dump mined containing 12.4 g/t of gold (Hussein, 1990). A gold vein-type mineralization is located structurally in NW-SE shear zones and is related to a gabbro-diorite intrusion. The gabbro-diorite associations were lightly metamorphosed into a metagabbro-diorite complex which exhibits irregular hydrothermal alteration stages. Auriferous veins are restricted to the contact between the olivine gabbro norite (younger intrusion). These mineralizations are related to the NW-SE faulting system and shearing (Abdelnasser and Kumral, 2017) with a gold content ranging from 2.2 to 25.7 g/t (El-Taher et al., 2003). Arsenopyrite, sphalerite, pyrite, chalcopyrite, tetrahedrite, and pyrrhotite are associated with the weathered host rocks and the mineralized quartz veins.

## 2.2 Climate

The desert region of Egypt is characterized by a dry

climate with extremely hot summers and mild winters with temperatures ranging between max 37°C (in July) and min 10°C (in January). The mean precipitation of about 5.5 mm/y occurs mainly during the winter. Flash flood events with high rainfall (~60 mm/h) can occur sporadically (Ghoneim et al., 2002).

## 3 Material and methods

### 3.1 Samples collection

The tailings were deposited around the mine localities and downstream in small wadis. They are characterized by small grain sizes. Two representative samples were collected from the first 10 cm-depth from the Fatira, El Sid, Barramiya and Atud tailings utilizing a stainless steel trowel and then placed in plastic bags. The Fatira tailings are characterized by pale yellow to beige color, while the Atud tailings have a whitish color. The colors of the El Sid tailings were pale yellow to gray with small desiccation cracks. The Barramiya tailings have gray-dark gray

color with beige varnish and deep desiccation cracks and much-enhanced erosion and channel washout. Different sample divisions were attained utilizing a sample splitter. The tailings were then examined for particle size, chemistry and mineralogy (Fig. 3).



**Fig. 3** Dry tailings stacks (a) in front of the mine with blocks of agglutinated, (b) tailings from Fatira. (c) Surface and (d) lateral views of El Sid gold mine tailings with the distribution of desiccation cracks. (e) Surface view, (f) high intensive subsidence channels of Barramiya gold mine tailings. Disseminated heaps (g, h) of whitish tailings from Atud area.

### 3.2 Sample analysis

#### 3.2.1 Grain size analysis

Grain size distribution was evaluated using a CAMSIZER (Retsch GmbH) for particle sizes over 63  $\mu\text{m}$ , and a SediGraph 5100 (Micromeritics Instrument Co) for particle sizes under 63  $\mu\text{m}$ .

#### 3.2.2 Powder analysis

An X-ray Fluorescence (XRF, PW1480/PW2400) was used for identifying the chemical compositions of major oxides (wt.%) and several trace metals and metalloids (like As, Cd, Co, Cr, Cu, Ni, Pb, Sr, V, and Zn in mg/kg). The bulk mineral identification of crystalline materials

was measured in the samples using X-ray powder diffraction patterns (XRD, PW3710) with monochromated  $\text{CuK}\alpha$  radiation. The operation condition was at 40 kV and 30 mA. A Galaxy software package was used for data evaluation.

#### 3.2.3 Environmental Scanning electron microscope (SEM)

Micro-textural identifications of the different phase identifications on polished thin sections developed from the powder samples were done using ESEM (FEI Quanta 650F ESEM) linked to an energy dispersive X-ray (EDS) detector (Bruker Nano GmbH).

## 4 Results and discussion

Like many countries with scarce water resources and arid climate, paste thickening discharge and high density technologies methods were used in tailings disposal. High density thickened tailings is a process that involve dewatering the tailings to a point, where they will form a homogeneous non-segregated mass with uniform grain size and mineralogy when deposited (Schoenbrunn and Bach, 2015). Rapid consolidation takes place within these tailings due to the high temperatures in the Eastern Desert.

### 4.1 Geochemical patterns

#### 4.1.1 Bulk rock chemistry

The investigated tailings samples show different bulk chemical compositions (Fig. 4, Table S1). The three dominant oxides in the tailings materials are  $\text{SiO}_2$ ,  $\text{Fe}_2\text{O}_3$ , and  $\text{Al}_2\text{O}_3$ . CaO is the third abundant oxide in the Atud tailings whereas  $\text{K}_2\text{O}$  is the third most abundant oxide in the Fatira tailings materials while it is the lowest in the Atud (Fig. 4(a)).  $\text{Al}_2\text{O}_3$  is the highest in Atud and Fatira and the lowest in El Sid tailings materials. MgO is high in Atud tailings and low in Fatira tailings. The chemical composition, therefore, shows that the Atud mine tailings material shows high acid neutralizing capacity due to its high calcite percentage compared to the other mine tailings (Fig. 4(b)).  $\text{Fe}_2\text{O}_3$  is enriched in the Fatira tailings compared to the other tailings materials. Most enrichment of Cr (mean 569 mg/kg), Ni (mean 89 mg/kg), and Co (mean 42 mg/kg) are concurring with the high MgO, and CaO, pointing toward mafic/ultramafic dominion (Garver et al., 1996) (olivine gabbro norites, serpentinites, talc-carbonates, and graphite schists) in the Atud and Barramiya tailings materials (mean 287, 191, and 21 mg/kg of Cr, Ni, and Co) (Fig. 4(c)). The tailings from El Sid are characterized by high values of Pb (mean 1349 mg/kg) and Zn (mean 1357 mg/kg), followed by the Fatira tailings that reflect the acidic nature of the host rocks. The Barramiya tailings have higher As values (mean

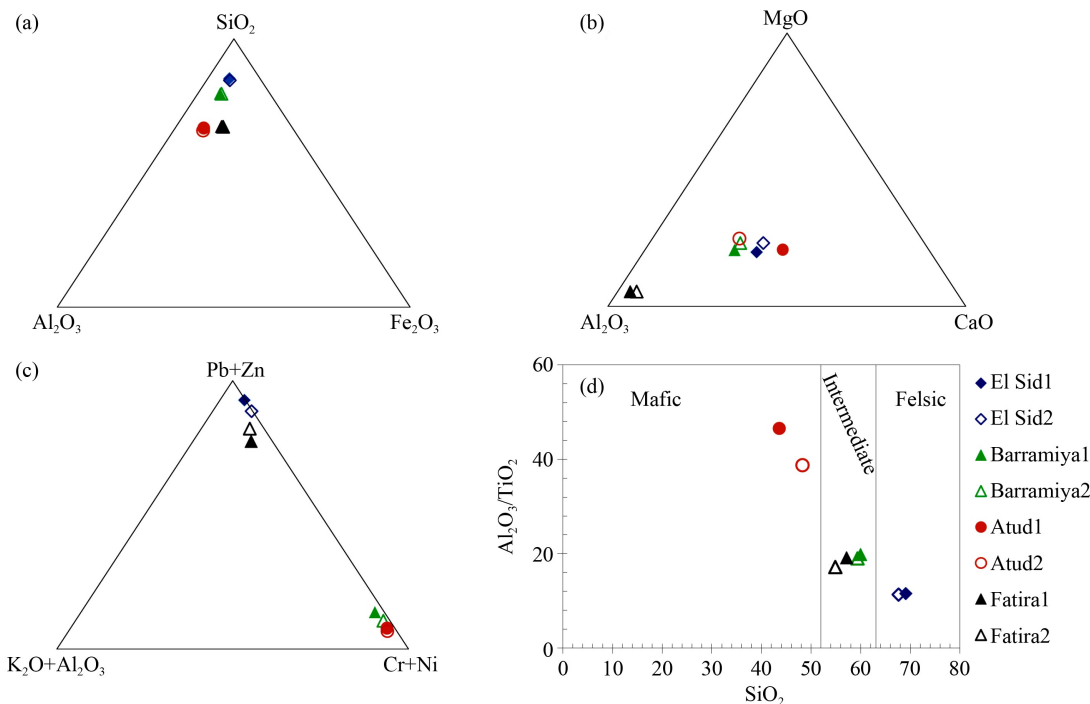


**Fig. 4** Triangular plot of (a) SiO<sub>2</sub>, Al<sub>2</sub>O<sub>3</sub>, and Fe<sub>2</sub>O<sub>3</sub>, (b) MgO, Al<sub>2</sub>O<sub>3</sub>, and CaO, (c) Pb+Zn, K<sub>2</sub>O+Al<sub>2</sub>O<sub>3</sub>, and Cr+Ni, bivariate diagram for (d) Al<sub>2</sub>O<sub>3</sub>/TiO<sub>2</sub> vs. SiO<sub>2</sub> showing mixing trends according to host rocks lithology (quartz vein, granite and mafics/ultramafics) of the tailings materials.

2635 mg/kg). The tailings from Fatira are characterized by a high concentration of Sr (mean 444 mg/kg) and Cu (mean 280 mg/kg) which indicates auriferous quartz (Harraz et al., 2012). The Sr enrichment in the Fatira tailings as opposed to the concentrations of alkaline earth metals (Ca and Mg) which are enriched in the Atud may be due to Sr adsorption to iron oxides such as hematite and goethite (Sahai et al., 2000; Nedobukh and Semeni-shchev, 2020) which showed greater concentration in the Fatira. The remarkably great loads of potentially hazardous elements such as Fe, As, Cu, Pb, and Zn in the tailings materials are due to the associated minerals pyrite, arsenopyrite, chalcopyrite, sphalerite, and galena in the ores. Ag, Au, As, Cu, Mo as well as Pb patterns are akin to the auriferous quartz mineralization (Harraz et al., 2012). The Al<sub>2</sub>O<sub>3</sub>/TiO<sub>2</sub> vs. SiO<sub>2</sub> plot of Le Bas et al. (1986) shows that the El Sid tailings materials are felsic in composition, the Atud tailings are of mafic composition while tailings from Barramiya and Fatira are intermediate in composition (Fig. 4(d)). Variations in the compositions of the tailings materials come from the mixing of the host rock lithology between granitic, quartz veins, schists, mafic, and ultramafic host rocks during the grinding and extraction of the gold (Redwan and Rammlmair, 2012).

## 4.2 Physical and mineralogical patterns

### 4.2.1 Particle-size distribution

The samples sizes are very fine due to the process of gold

extraction. The tailings materials are extremely poorly sorted. In El Sid, Barramiya and Fatira they are of silty size grains and clay with fine to very fine sands. The grain sizes in Atud increase to mainly consist of fine to coarse sands. The tailings materials of Barramiya are characterized by finer grain size distribution than the other tailings (Fig. 5). During flash flood events, the fine tailings materials suffer severe erosion due to their very fine particle sizes and the presence of the tailings materials downstream near the mine sites and in the middle of the wadis (Sadeghi et al., 2018; Redwan and Rammlmair, 2012; Redwan and Bamousa, 2019). This was evidenced by the presence of deeper and wider desiccation cracks within the Barramiya tailings.

### 4.2.2 Bulk mineralogy (XRD)

Quartz is the main constitute mineral in the Fatira tailings, in addition to other minerals like feldspars, calcite, hornblende, muscovite/illite, chlorite, and gypsum and goethite as secondary phases. These were crystallized after the precipitation of the tailings due to rapid evaporation of water (Harraz et al., 2012). Fatira shows a mixed granite nature with quartz veins and some mafics. An old mining dump from Fatira was studied by Naim et al. (1997). The dump consists mainly of quartz and alkali feldspars with minor magnetite, pyrite, goethite, and clay minerals from the feldspar alteration. The Barramiya tailings are characterized by quartz, muscovite/illite, dolomite, and feldspars with minor phases as

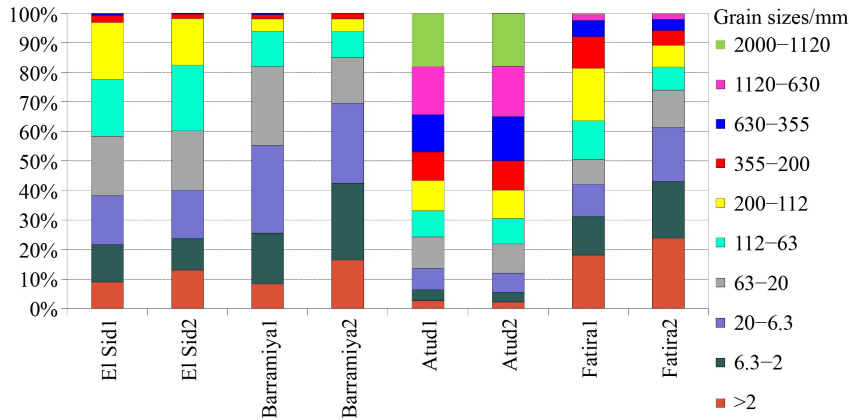


**Fig. 5** Grain size distribution (in mm) of the tailings samples from El Sid, Barramiya, Atud and Fatira.

greanalite and kaolinite arguing for variable constituents of mafic/ultramafic, schists, and quartz veins. Clay minerals are resultant from the feldspar alterations (Yuan et al., 2019). The El Sid tailings are characterized by the presence of quartz, calcite, biotite, chlorite, and feldspars reflecting the granite nature of the host rock during mining (Myers, 1997). In addition, there are minor amounts of ankerite, talc, and gypsum as a secondary crystallized phase. An old mining heap at El Sid consisted mainly of quartz, feldspar, biotite, and chlorite and minor galena, pyrite, chalcopryrite, sphalerite, goethite, and limonite (Naim et al., 1997). Hornblende, feldspars, chlorite, and calcite are predominant in the Atud tailings (Fig. 6).

4.2.3 Detailed mineralogy and heavy elements dispersion

The tailings materials are characterized by very small grain sizes, uniform distribution of their contents and variable minerals alteration. Few secondary mineral phases

are identified in the tailings materials from all areas due to incomplete sulfide oxidation as a result of the scarcity of water in Egypt. A mixture of metastable phases of Fe (oxy-)hydroxides and sulfates can develop in tailings environments contingent on the concentration of soluble species, the pH, and solution redox potential (Blowes and Ptacek, 2003). These efflorescent mineral phases frequently form as a result of the evaporation of Acid Mine Drainage (AMD) expelled from tailings, waste rock, or mine workings (Nordstrom and Alpers, 1999).

Incipient oxidation of pyrite is identified along the cracks and/or along the edges of the mineral particles (Figs. 7(b)–7(d)) from El Sid, Barramiya, and Atud. The sulfates contain amounts of Si, Al, Si, and Mg from the dissolution of the associated minerals. Fe sulfates change over time into the more thermodynamically stable crystalline iron oxides of goethite and hematite (Mayer and Jarrell, 1996; Jones et al., 2009). Gypsum and bassanite are the typical secondary minerals formed where evaporation exceeds precipitation on the surface layers of El Sid

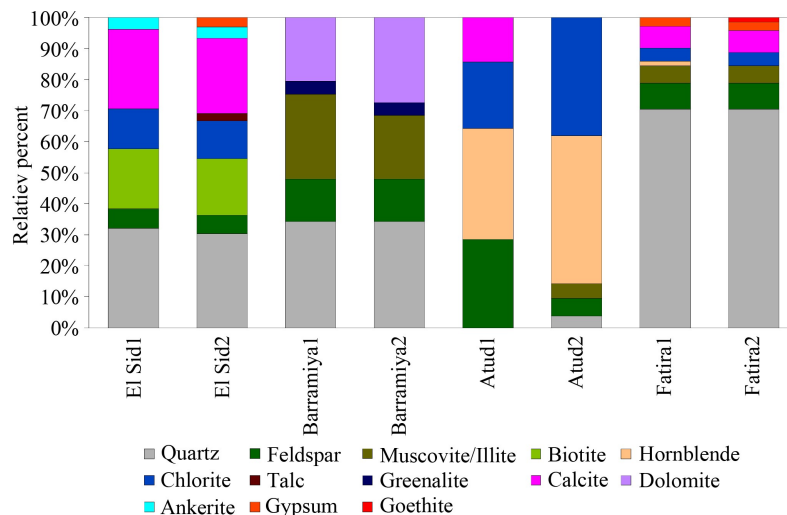


**Fig. 6** Rough estimate of relative mineral phase distribution depend on XRD measurements coded for major phases by order of intensity from 50 to 10, and for traces from 6 to 1 and afterwards accumulated to 100% on the basis of coding, of the tailings samples.

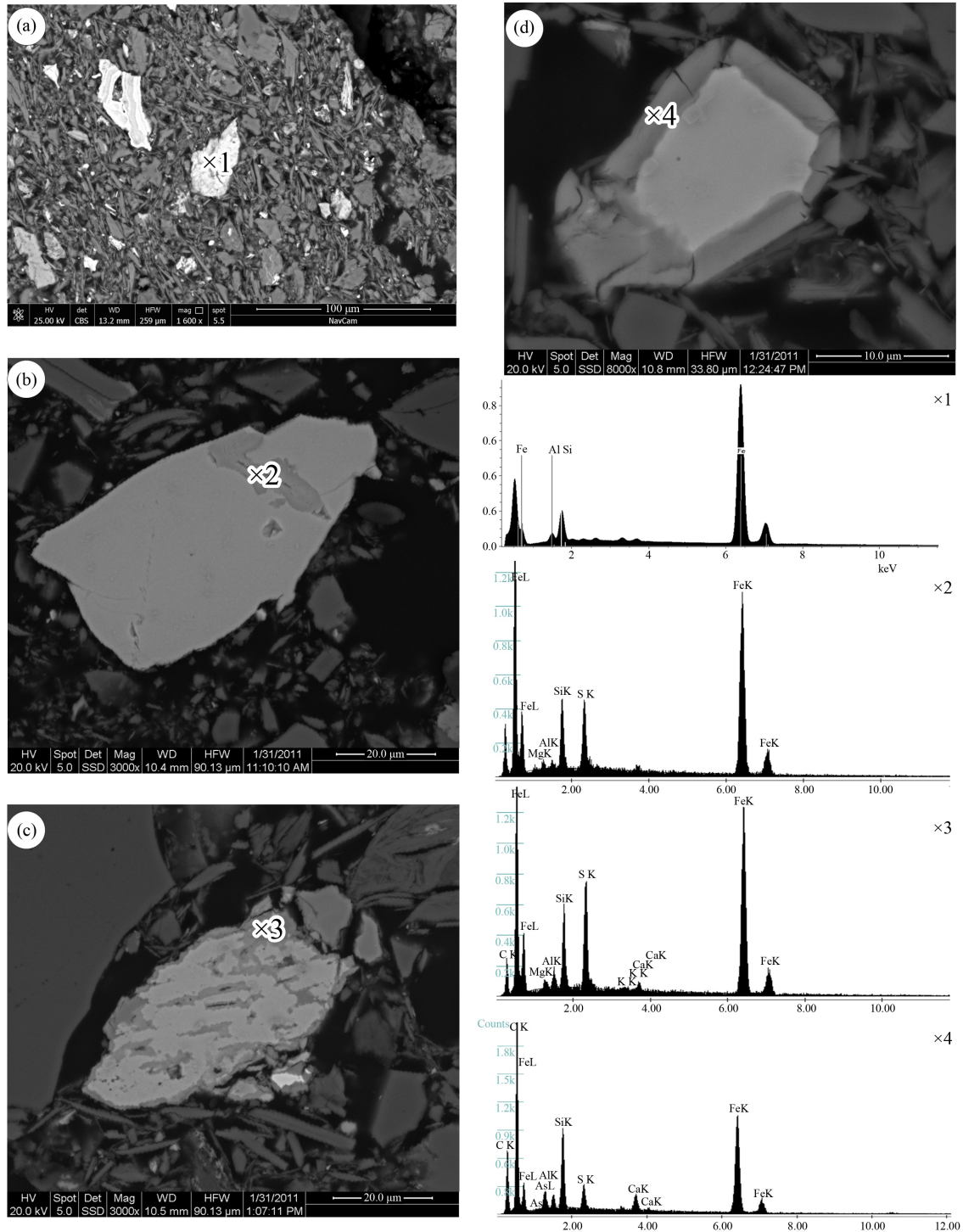


**Fig. 7** BSE images of a) finely ground tailings sample from Fatira mine rich in iron sulfates and Si, b) incipient pyrite alteration along the cracks filled by Si, Al, Si and Mg sulfates of El Sid tailings, c) pyrite alteration along the rims and cracks variable filled by Fe, Si, Al, Si and Mg sulfates from Barramiya tailings, d) Atud tailings with rim alteration rich in iron sulfates with variable Si and Al.

and Barramiya (Redwan and Rammlair, 2012) due to the abundant carbonate minerals of calcite, ankerite, and dolomite (Fig. 5). The occurrence of goethite at Fatira (Fig. 7(a)) may be the result of such a conversion process. Sorption onto or incorporation in the structure of these

$\text{Fe}^{3+}$  (oxy-)hydroxides and sulfates can be an essential control on the mobility and attenuation of heavy and trace elements in the tailings (Durocher and Schindler, 2011). There are limited occurrence and distribution of secondary minerals in these tailings.

In dry climates, where evaporation exceeds precipitation, the water-flow direction with the mobile elements in the tailings systems such as Ca, K, Na, SO<sub>4</sub>, and Cl, changes to upwards migration toward the top layers due to capillary transport forces (Zuddas, 2010). Supersaturation manages the precipitation of water-soluble secondary mineral sulfates (Dold and Fontboté, 2001). These unstable efflorescent phases enriched in metals undergo extreme erosion during heavy rainfalls and carry the heavy contaminant loads to the surrounding ecosystem.

Contamination through water pollution, aeolian dispersion, and contamination of the food chain near tailings impoundment are widespread worldwide. Excessive exposures give rise to numerous diseases in living organisms. The results acquired from the geochemical and mineralogical identification of the samples gathered from tailings permit recognizing the possible environmental concerns that would disturb the different mine areas. The threshold effect level (TEL) is introduced to evaluate the ecotoxicology caused by heavy metals in the tailings materials (Ma et al., 2015). The values of TEL for Zn, Cr, Pb, Cu, and As are 124, 52, 30, 19, and 5.9 mg/kg, respectively. The values of TEL indicate high possible impacts from heavy elements contamination to the surrounding ecosystem. High Pb poisoning induces renal failure and severe gastro-intestinal distress, kidney disease, hypertension, and anemia (Plumlee and Ziegler, 2003). Zn poisoning causes abdominal pain, nausea, and vomiting. Further effects may take into consideration lethargy, anemia, dizziness, and renal damage (Plum et al., 2010). Arsenic poisoning can result in diseases such as skin and lung cancer, diabetes, hematologic disorders, and cardiovascular disease (Centeno et al., 2007). Copper supplies essential micronutrients to plants, animals, and humans. Nevertheless, a higher Cu value may result in liver, and kidney renal tubular damage (Eom et al., 2020). A leak to the surrounding environment of these toxic elements could be disastrous for the local community and requires a well-defined mine site rehabilitation strategy from authorities for future evaluation.

## 5 Conclusions

The four studied gold mine tailings materials in the Eastern Desert of Egypt are characterized by very fine silty particle sizes with very fine sands and clays in El Sid, Barramiya, and Fatira, and fine to coarse sands in Atud. SiO<sub>2</sub>, Fe<sub>2</sub>O<sub>3</sub>, and Al<sub>2</sub>O<sub>3</sub> are the main oxides in the tailings materials. CaO is abundant in Atud whereas K<sub>2</sub>O is an abundant oxide in the Fatira and lowest in Atud. Al<sub>2</sub>O<sub>3</sub> is highest in Atud and Fatira and lowest in the El Sid tailings. Fe<sub>2</sub>O<sub>3</sub> is enriched in the Fatira tailings. High mean values of Cr, Ni, and Co are coinciding with the mafic/ultramafic nature in the Atud and Barramiya tailings. The El Sid tailings are characterized by higher mean values of Pb and Zn. The Barramiya tailings have a higher mean As concentration. The tailings from Fatira are characterized by high mean values of Sr and Cu resulting from the auriferous quartz mineralization. Sr enrichments in the Fatira tailings are due to their adsorption to iron oxides.

Quartz is the main component in all tailings. The Fatira tailings contain feldspars, calcite, hornblende, muscovite/illite, chlorite, gypsum, and goethite. Barramiya tailings include muscovite/illite, dolomite, and feldspars. The El Sid tailings are characterized by the presence of calcite, biotite, chlorite and feldspars. Hornblende, feldspars, chlorite, and calcite are predominant in the Atud tailings.

As a result of the insufficient water in Egypt, the ESEM-EDS analysis identified incipient oxidation of pyrite along the cracks and/or along the edges of the particles in El Sid, Barramiya, and Atud. The values of TEL indicate high possible impacts from heavy metal contamination to the surrounding ecosystem. The tailings were deposited downstream in small wadis. Crucial environmental hazards are related to different main routes (water flows and wind erosion) that can involve efflorescent materials enriched in potentially toxic elements e.g. As, Pb, and Zn at the top surface. Such abandoned tailings deposits need to be outlined, monitored, and restored in order to evade the mobilization of large volumes of potentially hazardous elements.

## Appendix A.

**Table S1** Chemical composition of tailings materials measured using XRF

oxide/element	El Sid1	El Sid2	Barramiya1	Barramiya2	Atud1	Atud2	Fatira1	Fatira2
SiO <sub>2</sub> /%	69.12	67.64	60.03	59.33	43.6	48.24	57	54.85
TiO <sub>2</sub> /%	0.611	0.627	0.54	0.541	0.4	0.489	1	0.926
Al <sub>2</sub> O <sub>3</sub> /%	7.03	7.11	10.69	10.28	16.5	18.95	17	15.89
Fe <sub>2</sub> O <sub>3</sub> /%	5	5.3	4.76	5.03	5.3	6.18	11	10.92
MnO/%	0.107	0.115	0.12	0.112	0.1	0.108	0	0.054
MgO/%	2.88	3.67	4.07	4.64	8.4	9.25	1	0.97

(continued)

oxide/element	El Sid1	El Sid2	Barramiya1	Barramiya2	Atud1	Atud2	Fatira1	Fatira2
CaO/%	4.578	5.027	4.926	5.069	15.5	9.059	1	0.936
Na <sub>2</sub> O/%	1.66	1.22	1.06	1.12	1.3	1.07	1	2.10
K <sub>2</sub> O/%	1.464	1.522	1.916	1.706	0.2	0.222	5	4.384
P <sub>2</sub> O <sub>5</sub> /%	0.212	0.2	0.064	0.068	0.0	0.049	0	0.257
(SO <sub>3</sub> )/%	2.12	1.85	0.89	0.62	0.3	0.02	0	0.34
(Cl)/%	0.027	0.027	0.011	10.8	0.1	0.018	0	0.012
(F)/%	0.1	0.12	<0.05	<0.05	<0.05	<0.05	0	0.14
LOI/%	4.35	4.84	10.17	10.8	8.0	6.03	6	7.96
Sum/%	99.26	99.27	99.29	99.34	99.62	99.69	100	99.74
(As)/(mg·kg <sup>-1</sup> )	1078	1278	3092	2178	14	14	45	45
Ba/(mg·kg <sup>-1</sup> )	348	333	297	253	46	41	654	609
Ce/(mg·kg <sup>-1</sup> )	57	42	41	60	41	<18	<52	<52
Co/(mg·kg <sup>-1</sup> )	15	16	19	23	42	41	7	11
Cr/(mg·kg <sup>-1</sup> )	125	187	240	334	560	578	47	51
Cu/(mg·kg <sup>-1</sup> )	43	41	48	45	67	38	300	260
Ni/(mg·kg <sup>-1</sup> )	94	123	154	228	108	70	12	18
Pb/(mg·kg <sup>-1</sup> )	1446	1251	8	7	17	9	35	<6
Rb/(mg·kg <sup>-1</sup> )	38	41	48	43	7	7	114	108
Sc/(mg·kg <sup>-1</sup> )	8	10	18	16	34	34	17	<17
Sr/(mg·kg <sup>-1</sup> )	185	196	250	228	264	212	423	465
V/(mg·kg <sup>-1</sup> )	72	77	131	111	118	128	120	113
W/(mg·kg <sup>-1</sup> )	42	29	6	5	<4	<4	10	<8
Y/(mg·kg <sup>-1</sup> )	18	16	26	27	13	15	17	13
Zn/(mg·kg <sup>-1</sup> )	1477	1236	57	61	41	39	241	405
Zr/(mg·kg <sup>-1</sup> )	113	106	87	96	40	38	135	133

**Acknowledgments** Constructive criticisms of anonymous reviewers have improved the quality of the earlier version of the manuscript and are gratefully acknowledged.

## References

- Abd El Monsef M, Slobodnik M, Salem I A (2020). Characteristics and nature of gold-bearing fluids in Fatira area, North Eastern Desert of Egypt: possible transition from intrusion-related to orogenic deposits. *Arab J Geosci*, 13(19): 1034
- Abdelnasser A, Kumral M (2017). The nature of gold-bearing fluids in Atud gold deposit, Central Eastern Desert, Egypt. *Int Geol Rev*, 59(15): 1845–1860
- Attia M I (1948). Geology of the Barramiya Mining District. Cairo: Geological Survey of Egypt: 1–76
- Azzaz S A, Sabet A H, Soliman M M, Botros N S (1997). Mode of occurrence and genesis of the gold mineralizations in the North Eastern Desert of Egypt. *Egyptian Mineral*, 9: 169–185
- Blowes D W, Ptacek C J (2003). Mill tailings hydrogeology and geochemistry. In: Jambor J L, Blowes D W, Ritchie A I M, eds. *Environmental Aspects of Mine Wastes*. Mineral Assoc Canada Short Course Series 31, 95–116
- Blowes D W, Ptacek C J, Jambor J L, Weisener C G (2003). The Geochemistry of Acid Mine Drainage. In: Holland H D, Turekian K K, eds. *Treatise on Geochem* Pergamon, 149–204
- Botros N S (2004). A new classification of the gold deposits of Egypt. *Ore Geol Rev*, 25(1–2): 1–37
- Carmo F F, Lanchotti A O, Kamino L H Y (2020). Mining waste challenges: environmental risks of gigatons of mud, dust and sediment in megadiverse regions in Brazil. *Sustainability*, 12(20): 8466
- Centeno J A, Tseng C H, Van der Voet G B, Finkelman R B (2007). Global impacts of geogenic arsenic: a medical geology research case. *Ambio*, 36(1): 78–81
- Dold B, Fontboté L (2001). Element cycling and secondary mineralogy in porphyry copper tailings as a function of climate, primary mineralogy, and mineral processing. *J Geochem Explor*, 74(1–3): 3–55
- Durocher J L, Schindler M (2011). Iron-hydroxide, iron-sulfate and hydrous-silica coatings in acid-mine tailings facilities: a comparative study of their trace-element composition. *Appl Geochem*, 26(8): 1337–1352
- El-Bouseily A M, El-Dahhar M A, Arslan A I (1985). Ore-microscopic and geochemical characteristics of gold-bearing sulfide minerals, El Sid Gold Mine, Eastern Desert, Egypt. *Mineral Depos*, 20(3):

- 194–200
- El Ramly M F, Ivanov S S, Kochin G C, Bassyouni F A, Abdel Aziz A T, Shalaby I M, El Hammady M Y (1970). The occurrence of gold in the Eastern Desert of Egypt. In: Moharram O, Gachechiladze D Z, El Ramly M F, Ivanov S S, Amer A F, eds. *Studies on Some Mineral Deposits of Egypt. Part I, Sec. A, metallic minerals*, Geol Surv Egypt, 21: 53–64
- El-Taher A, Kratz K L, Nossair A, Azzam A H (2003). Determination of gold in two Egyptian gold ores using instrumental neutron activation analysis. *Radiat Phys Chem*, 68(5): 751–755
- Eom S Y, Yim D H, Huang M, Park C H, Kim G B, Yu S D, Choi B S, Park J D, Kim Y D, Kim H (2020). Copper-zinc imbalance induces kidney tubule damage and oxidative stress in a population exposed to chronic environmental cadmium. *Int Arch Occup Environ Health*, 93(3): 337–344
- Gabra S (1986). Gold in Egypt: a commodity package, minerals, petroleum and groundwater assessment program: USAID project 363–0105. *Geol Surv Egypt*
- Garver J I, Royce P R, Smick T A (1996). Chromium and nickel in shale of the Taconic foreland: a case study for the provenance offine-gained sediments with an ultramafic source. *J Sediment Res*, 66: 100–106
- Ghoneim E M, Arnell N W, Foody G M (2002). Characterizing the flash flood hazards potential along the Red Sea coast of Egypt. *IAHS Publ*, 271: 211–216
- Harraz H Z, Hamdy M M, El-Mamoney M H (2012). Multi-element association analysis of stream sediment geochemistry data for predicting gold deposits in Barramiya gold mine, Eastern Desert, Egypt. *J Afr Earth Sci*, 68: 1–14
- Helser J, Cappuyns V (2021). Trace elements leaching from Pb-Zn mine waste (Plombières, Belgium) and environmental implications. *J Geochem Explor*, 220: 106659
- Hudson-Edwards K A, Jamieson H E, Lottermoser B G (2011). Mine wastes: past, present, future. *Elements*, 7(6): 375–380
- Hussein A A (1990). Mineral deposits. In: Said R, ed. *The Geology of Egypt*. Rotterdam: Balkema, 511–566
- Jones A M, Collins R N, Rose J, Waite T D (2009). The effect of silica and natural organic matter on the Fe(II)-catalysed transformation and reactivity of Fe<sup>3+</sup> minerals. *Geochim Cosmochim Acta*, 73(15): 4409–4422
- Klemm D, Klemm R, Murr A (2001). Gold of the Pharaohs—6000 years of gold mining in Egypt and Nubia. *J Afr Earth Sci*, 33(3–4): 643–659
- Klemm R, Klemm D (2013). *Gold and Gold Mining in Ancient Egypt and Nubia*. Berlin: Springer-Verlag
- Kochin G G, Bassyuni F A (1968). Mineral resources of the UAR. Report on the generalisation of geologic data on mineral resources in the UAR, carried out under contract 1247 (1966 to 1968), part I: Metallic minerals. Internal Report 18/68, Geol Surv Egypt
- Le Bas M J, Le Maitre R W, Streckeisen A, Zanettin B (1986). A chemical classification of volcanic rocks based on the total alkali-silica diagram. *J Petrol*, 27(3): 745–750
- Ma Y Q, Qin Y W, Zheng B H, Zhang L, Zhao Y M (2015). Seasonal variation of enrichment, accumulation and sources of heavy metals in suspended particulate matter and surface sediments in the Daliao river and Daliao river estuary, northeast China. *Environ Earth Sci*, 73(9): 5107–5117
- Myers J S (1997). Geology of granite. *J R Soc West Aust*, 80(3): 87–100
- Mayer T D, Jarrell W M (1996). Formation and stability of iron(II) oxidation products under natural concentrations of dissolved silica. *Water Res*, 30(5): 1208–1214
- Mendez M O, Maier R M (2008). Phytostabilization of mine tailings in arid and semiarid environments—an emerging remediation technology. *Environ Health Perspect*, 116(3): 278–283
- Murr A (1999). Genesis of the gold deposit districts of Fatira, Gidami, Atalla and Hangaliya in the Egyptian Eastern Desert, *Münchner Geol. Hefte A* 27, 203 pp (in German)
- Naim G M, Hassan A K, El-Sirty E A, Mansour A M, Dardir A A, Rasmy A H, Eskander M Z (1997). Project of economic evaluation and methods of treatment for dump and tailing of the old Egyptian gold mines. In: *Geol Surv Egypt Documentation center* (in Arabic)
- Nedobukh T A, Semenishchev V S (2020). Strontium: source, occurrence, properties, and detection. In: Pathak P, Gupta D, eds. *Strontium Contamination in the Environment. The Handbook of Environmental Chemistry*, vol 88. Berlin: Springer Verlag
- Nordstrom D K, Alpers C N (1999). Geochemistry of acid mine waters. In: Plumlee G S, Logsdon M J, eds. *The Environmental Geochemistry of Mineral Deposits, Reviews in Economic Geology*, vol. 6A, Society of Economic Geologists Inc Littleton, Colorado, USA, 133–160
- Plum L M, Rink L, Haase H (2010). The essential toxin: impact of zinc on human health. *Int J Environ Res Public Health*, 7(4): 1342–1365
- Plumlee G S, Ziegler T L (2003). The medical geochemistry of dusts, soils, and other earth materials. In: Lollar B S, Holland H D, Turekian K K, eds. *Treatise on Geochemistry*. Elsevier Publ, 9: 263–310
- Redwan M, Bamoussa A O (2019). Characterization and environmental impact assessment of gold mine tailings in arid regions: a case study of Barramiya gold mine area, Eastern Desert, Egypt. *J Afr Earth Sci*, 160: 103644
- Redwan M, Rammlmair D (2012). Influence of climate, mineralogy and mineral processing on the weathering behaviour within two, low-sulfide, high-carbonate, gold mine tailings in the Eastern Desert of Egypt. *Environ Earth Sci*, 65: 2179–2193
- Sadeghi S H, Gharemahmudli S, Kheirfam H, Khaledi Darvishan A, Kiani Harchegani M, Saeidi P, Gholami L, Vafakhah M (2018). Effects of type, level and time of sand and gravel mining on particle size distributions of suspended sediment. *Int Soil Water Conserv Res*, 6(2): 184–193
- Sahai N, Carroll S A, Roberts S, O'Day P A (2000). X-ray absorption spectroscopy of strontium (II) coordination II: sorption and precipitation at kaolinite, amorphous silica, and goethite surfaces. *J Colloid Interf Sci*, 222(2): 198–212
- Schoenbrunn F, Bach M (2015). The development of paste thickening and its application to the minerals industry; an industry review. *Berg Huettenmaenn Monatsh*, 160(6): 257–263
- Souissi R, Souissi F, Ghorbel M, Munoz M, Courjault-Radé P (2015). Mobility of Pb, Zn and Cd in a soil developed on a carbonated bedrock in a semi-arid climate and contaminated by Pb–Zn tailing, Jebel Ressa (NE Tunisia). *Environ Earth Sci*, 73(7): 3501–3512
- Yuan G, Cao Y, Schulz H M, Hao F, Gluyas J, Liu K, Yang T, Wang Y, Xi K, Li F (2019). A review of feldspar alteration and its geological significance in sedimentary basins: from shallow aquifers to deep hydrocarbon reservoirs. *Earth Sci Rev*, 191: 114–140
- Zuddas P (2010). Water-rock interaction processes seen through thermodynamics. *Elements*, 6(5): 305–308